Available online at www.garmian.edu.krd

Passer Journal of Basic and Applied Sciences

Passer 7 (Issue 1) (2025) 90-99

Original Article

Vibration Analysis of Porous Axially Graded Pipe Conveying Fluid on the Pasternak foundation

Zahraa Qassim Jerad [1], Talib Ehraize Elaikh [*1], Ahmed Abdul-Hussein Ouda[1]

[1]*Department of Mechanical Engineering, College of Engineering, University of Thi-Qar, Thi-Qar, 64001, Iraq.*

Received 21 Nowember 2024; revised 1 January 2025;
accepted 21 February 2025; available February 25 February 2025

DOI: 10.24271/PSR.2025.489929.1822

ABSTRACT

This paper investigates the stability of an axially functionally graded (AFG) pipe carrying fluid supported by two elastic foundations and constrained by double-clamped end conditions. The Hamilton principle provides the vibration equations, while the Galerkin procedure discretizes the system equation to facilitate dynamic behaviour analysis. Mechanical properties of the pipe vary axially following a power-law distribution. The effect of material gradients, porosities, boundary conditions, elastic foundation properties, and flow velocity on pipe stability is investigated. The present study results are compared to the existing literature for homogeneous pipes on elastic foundations. The results show that stability increases with higher foundation stiffness and Young's modulus ratio, decreasing as the axial gradient and porosity coefficients increase.

Keywords: (AFGP), Natural frequency, Critical velocity, Porosity, Galerkin method (GM).

1 Introduction

The vibration behaviour of fluid-conveying pipes exemplifies fluid-solid coupling phenomena. These structures have extensive applications in various engineering sectors, such as marine engineering, nuclear power, aerospace, and petrochemical industries. Thus, studying the dynamics of these systems holds substantial engineering and academic significance, making them a topic of considerable interest to researchers [1]. (Giacobbi et al.) [2] utilized the finite element (FE) method to inspect the impact of longitudinally varying density on the dynamics behaviour of pipes flowing fluid with clamped and cantilevered boundary conditions. A dynamic analysis of Rayleigh pipes with flowing fluid and non-classical boundary conditions was carried out by [3]. (Xu et al.) [4] computed the complex vibration of a viscoelastic fluid-conveying clamped pipe using the Differential Quadrature (DQ) Method. (Q. Zhao et al.) [5] employed DTM and Galerkin distributions to conduct the dynamics of the pipe-carrying fluid.

In petroleum engineering, pipelines frequently traverse challenging terrains, including sand, gravel, soil, and mixed environments, during the conveyance of oil and gas. Therefore, the flow of oil or gas through these pipes in challenging environments makes them susceptible to unstable vibrations [6]. Consequently, much interest has been generated in studying the stability of pipes conveying fluid supported by elastic foundations under various boundary conditions. (Y. Ma et al.) [6] investigated the vibration stability of a pipe-carrying fluid supported by a two-parameter foundation using the harmonic differential quadrature (HDQ) method. (M. Li et al.) [7] utilized Green's function to obtain an explicit solution for the vibrations of oil-conveying pipes supported by Pasternak foundations. Askarian et al., 2020 [8] examined the stability of pipes translating fluid lying on a viscoelastic foundation. The pipe motion equation was acquired using the concepts of Hamilton and solved through the Galerkin method. (Balkaya and Orhan Kaya) [9] studied the stability of the pipe lying over the Winkler-Pasternak foundation. Using the semi-analytic solution (DTM), they determined the system's critical velocities and complex frequencies. (Wu et al.) [10] proposed the dynamic stiffness (DS) method for examining the impact of Pasternak foundation parameters on the stability of pipes that convey fluid across multiple spans.

* Corresponding author
E-mail address talib-h@utq.edu.iq (Instructor).
Peer-reviewed under the responsibility of the University of Garmian.

Additionally, functionally graded materials (FGMs) are innovative composite materials with properties that gradually change across spatial positions, enabling the customization of material characteristics by controlling the distribution of volume fractions, and these materials exhibit significantly enhanced performance over conventional materials, particularly in fracture toughness and wear resistance [11]. In this regard, most research on FGMs has focused on beams, plates, and shells (Awrejcewicz et al.; T. E. Elaikh et al.; Jha et al.) [12-14], with comparatively limited studies addressing the dynamic behaviour of FGM pipelines used for fluid transport. (Cao) [15] conducted the impact of random foundations on the critical velocity of FGM pipes under thermal stress using (FEM). (T. Ma and Mu) [16] determined the influence of multiple physical fields on the stability of FGM simply-supported microtubes. The governing equation for these microtubes was obtained using Hamilton's principle with conjugate of strain gradient theory. (Guo et al.) [17] proposed an effective statistical method for flow pipeline systems constructed with random axial gradient materials. (Ihmood et al.) [18] studied the stability of fluid-flow pipes made of new inhomogeneous materials. (R. B et al.) [19] established a linear vibration model of FGM flow pipes on visco-elastic foundations. The linear frequency and stability were determined using DQM. (Selmi and Hassis) [20] analyzed the vibration of the fluid-conveying pipeline made of functional gradient materials using the exact solution for various end conditions. (Deng et al.) [21] studied the stability of viscoelastic functional gradient material pipelines. Their research focused on the influence of volume fraction index, fluid velocity, and internal damping on the pipeline system's dynamics. (Wang and Liu) [22] studied the impact of gradient material indexes on the lateral vibration of pipeline conveying fluid. (An and Su) [23] used the generalized integral (GI) transform technique to numerically study the dynamic behaviour of the axial functional gradient pipeline conveying fluid. Y. Zhao et.) [24] investigated the vibration characteristic of functionally graded conical fluid-conveying pipes utilizing DQM. (T. E. H. Elaikh et al.) [25] addressed the natural frequency of FGM double micro-pipelines using the Galerkin method.

On the other hand, pores and micropores can form in functionally graded materials during the manufacturing process, which may negatively affect the mechanical characteristics of the structures. However, when the porosity distribution is optimized, it can enhance mechanical and structural properties such as energy dissipation, strength, and stiffness [26]. Consequently, porous functionally graded material pipelines for fluid transport have been widely utilized in engineering applications, such as nuclear reactors and aerospace. Nevertheless, limited research has been conducted to investigate the impact of these pores on the linear or nonlinear response of fluid-conveying FGM pipelines. (N. Li et al.) [27] employed the multiple-scale method to examine the nonlinear resonance of porous FGM pipes translating fluid. (Zhou et al.) [28] examined the influence of porosities on the dynamic response of fluid-conveying porous pipes made of radially graded materials. (Khodabakhsh et al.) [29] calculated the nonlinear stability of FGM Timoshenko model pipelines with uniform porosity and variable end conditions using an exact closed-form solution.

In the reviews above, it has been observed that most researchers have focused on the vibration analysis of composite pipes with radius gradients. According to the authors, the dynamic behaviour of functionally graded (FG) pipes with longitudinal gradients resting on an elastic foundation and containing porosity has not yet been studied. Therefore, this article addresses this gap by investigating the dynamic characteristics of fluid-conveying pipes graded in the axial direction. Then, a theoretical model is developed, and dynamic equations are extracted by applying Hamilton's precept. The solution method of vibration analysis is explained utilizing the Galerkin technique. The effects of foundation parameters, gradient index, flow velocity, and modulus ratio on vibration frequencies and stability are explored.

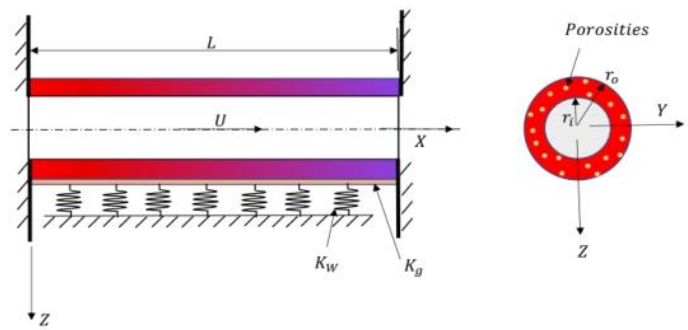

2 Mathematical Formulation

The clamped-clamped AFG pipe carrying fluid is shown in Figure 1. The length of the pipe is L. The inner and outer radius of the pipe are denoted by $r_i\ and\ r_o$, respectively, while U represents the fluid flow velocity inside the pipe.

Figure 1: Scheme diagram of clamped-clamped AFG porosity pipe.

2.1 Axially Graded Pipe Properties

This paper assumes that the FGM pipe material characteristics exhibit axial grading with uniform porosity, governed by a power-law function in which the physical characteristics progressively change from one end of the pipe to the other, as described by [30],

$$E(x) = E_0 E_X \tag{1}$$

$$\rho(x) = \rho_0 \rho_X \tag{2}$$

In which,

$$E_X = 1 + (\bar{\alpha}_E - 1)(\xi)^k - \frac{\lambda}{2}(\bar{\alpha}_E + 1), \tag{3}$$

$$\rho_X = 1 + (\bar{\alpha}_\rho - 1)(\xi)^k - \frac{\lambda}{2}(\bar{\alpha}_\rho + 1), \tag{4}$$

In this context, $(\bar{\alpha}_E = E_R/E_0)$ and $(\bar{\alpha}_\rho = \rho_R/\rho_0)$ represent the modulus and density ratios of the pipe's material properties, respectively. The indices o and L identify the left and right pipe sides; k is a positive value describing the variation in material along the pipe's length; λ denotes the porosity factor.

2.2 Governing Equations

The displacements u_x, u_y and u_z Along directions of X, Y, and Z for any point of the pipe are determined as outlined by [28].

$$\left.\begin{aligned} u_x(x,z,t) &= u(x,t) - z\,\frac{\partial w\,(x,t)}{\partial x} \\ u_y(x,z,t) &= 0 \\ u_z(x,z,t) &= w(x,t) \end{aligned}\right\} \tag{5}$$

In relation (5), w is the displacement of the pipe's middle plane, while t denotes the time.

Accordingly, the longitudinal strain resulting from pipe displacement can be expressed as:

$$\varepsilon_{xx} = \frac{\partial u}{\partial x} + \frac{1}{2}\left(\frac{\partial w}{\partial x}\right) - z\frac{\partial^2 w}{\partial x^2}$$
(6)

where z is the neutral fiber plane coordinate. Pipelines with elastic properties have the following stress-strain relationship::

$$\sigma_{xx} = E(x)\varepsilon_{xx} \tag{7}$$

An expression for the strain energy of FG pipelines is written as:

$$U = \int_V \sigma_{xx}\varepsilon_{xx} dV. \tag{8}$$

By inserting Equations (1), (6), and (7) in Equation (8), one can obtain:

$$U = \frac{1}{2}\int_0^L \left\{ E(x)A\left(\frac{\partial u}{\partial x} + \frac{1}{2}\left(\frac{\partial w}{\partial x}\right)^2\right)^2 + E(x)\,I\left(\frac{\partial^2 w}{\partial x^2}\right)^2 \right\} \mathrm{dx} \tag{9}$$

where A is the pipeline cross-sectional area, and I is the pipeline section's 2nd moment of area. The kinetic energy of the system is calculated as follows:

$$T = \frac{1}{2} m_f \int_0^L \left[\left(v + \frac{\partial u}{\partial x} + v\frac{\partial u}{\partial x}\right)^2 + \left(\frac{\partial w}{\partial t} + v\frac{\partial w}{\partial t}\right)^2\right] dx + \frac{1}{2}\int_0^L \rho(x)A\left[\left(\frac{\partial u}{\partial t}\right)^2 + \left(\frac{\partial w}{\partial t}\right)^2\right] dx \tag{10}$$

Further, the reaction force of the Pasternak Foundation performs virtual work as follows:

$$\delta W = \int_0^L \left(-k_W w + k_g \frac{\partial^2 w}{\partial x^2}\right)\delta w\, dx \tag{11}$$

where k_W and k_g Stand for Winkler and Pasternak stiffness coefficients, respectively. The dynamic equations of the pipe can be obtained by enforcing Hamilton's generalized law:

$$\delta \int_{t1}^{t2} (T - U + W)dt = 0 \tag{12}$$

By replacing the kinetic energy, potential, and work of the external force in equation (12), the equilibrium equations will be obtained as follows:

$$\frac{\partial^2}{\partial x^2}\left[E(x)I\frac{\partial^2 w}{\partial x^2}\right] + \left(m_f + \rho(x)A\right)\frac{\partial^2 w}{\partial t^2} + 2m_f v\frac{\partial^2 w}{\partial x \partial t} + m_f v^2\frac{\partial^2 w}{\partial x^2} + k_w w - k_p\frac{\partial^2 w}{\partial x^2} = 0 \tag{13}$$

The boundary condition equation for C-C is written as:

$$\left.\begin{aligned} w(0,t) &= \frac{\partial w(0,t)}{\partial x} = 0, \qquad at\ \ x = 0 \\ w(L,t) &= \frac{\partial w(L,t)}{\partial x} = 0, \qquad \text{at}\ \ x = L \end{aligned}\right\} \tag{14}$$

To simplify, these equations can be rewritten in dimensionless by

placing these parameters in Equation (13), the dimensionless system's equations will be obtained:

$$\frac{\partial^2}{\partial \xi^2}\left(E_X\frac{\partial^2 \eta}{\partial \xi^2}\right) + (u^2 - K_G)\frac{\partial^2 \eta}{\partial \xi^2} + 2\sqrt{\beta}u\frac{\partial^2 \eta}{\partial \xi \partial \tau} + K_W\eta + (\beta + (1 - \beta)\,\rho_X)\frac{\partial^2 \eta}{\partial \tau^2} = 0 \tag{16}$$

The boundaries (Equation 14) are also written in a dimensionless way as follows:

$$\left.\begin{aligned} At\ \ \xi = 0 \rightarrow \eta(\xi) = 0, \frac{\partial \eta(\xi)}{\partial \xi} = 0 \\ At\ \ \xi = 1 \rightarrow \eta(\xi) = 0, \frac{\partial \eta(\xi)}{\partial \xi} = 0 \end{aligned}\right\} \tag{17}$$

2.3 Method of Solution

Galerkin's method will be employed to find the vibration characteristics of the AFGM pipe. Through this method, the system equation (16) is transformed into an ordinary differential (OD) equation, and we can assume the displacement function $\eta(\xi,\tau)$ of the FG pipe as [31, 32],

$$\eta(\xi,\tau) = \sum_{j=1}^{N} \emptyset_j(\xi) q_j(\tau) \tag{18}$$

where N is the mode number to be considered, $q_j(\tau)$ is the time-dependent function, and $\emptyset_j(\xi)$ is the eigenfunction of the pipe.

The mode shape standards for the S-S boundary condition are provided as follows[33],

$$\emptyset_j(\xi) = \sqrt{2}\,sin\,(\,n\pi\,\xi) \tag{19}$$

Substituting equation (18) into equation (16) and multiplying the resulting expression by $\emptyset_k(\xi)$, and then integrating the obtained expression for x from zero to L, the system equation is obtained in general matrix form [34,35]:

$$[M]_{NxN}\,\ddot{q} + [C]_{NxN}\,\dot{q} + [K]_{NxN}\,q = 0 \tag{20}$$

in which

$$[M]_{jk} = \int_0^1 (\beta + (1-\beta)\,\rho_X)\,\emptyset_j(\xi)\emptyset_k(\xi)\,d\xi$$

$$[C]_{jk} = 2\sqrt{\beta}u\,\int_0^1 \emptyset_j^{(1)}(\xi)\emptyset_k(\xi)\,d\xi \tag{21}$$

$$[K]_{jk} = \int_0^1 E_X\emptyset_j^{(4)}(\xi)\emptyset_k(\xi)\,d\xi + 2\int_0^1 E_X'\emptyset_j^{(3)}(\xi)\emptyset_k(\xi)d\xi + \int_0^1 E_X^{(2)}\emptyset_j^{(2)}(\xi)\emptyset_k(\xi)\,d\xi + \left(u^2 - K_g\right)\int_0^1 \emptyset_j^{(2)}(\xi)\emptyset_k(\xi)\,d\xi + K_w\int_0^1 \emptyset_j(\xi)\emptyset_k(\xi)\,d\xi$$

Equation (21) is transformed into a first-order state equation, facilitating the solution of all system modes using MATLAB software. The dynamic characteristics equation of the system is evaluated through eigenvalue analysis. In this context, the eigenfrequency is expressed as a complex value (i.e., real and imaginary component): the real part represents the system's damping, while the imaginary part corresponds to its frequency.

3 Results and Discussion

This section elucidates the impact of foundation parameters, density variations, and material gradations along the pipe length on the system's stability behaviour at the clamped boundaries. It also presents a comparative study to assess the accuracy of the proposed method.

In the analytical examples, the geometric parameters for the AFG pipe are consistent with those specifi $\rho_f = 1000\ kg/m^3$ m, h=8 mm, and L=15m. The fluid density is . In this paper, the FG pipe comprises titanium (Ti-6Al-4V) on the left side and silicon (SiC) on the right. The properties of these materials are listed in Table 1.

Table 1: Axially functionally graded pipe material properties [36].

Materials	$E\,(GPa)$	$\rho_p\,(kg/m^3)$	$G\,(G\,Pa)$
SiC	440	3210	188
$Ti-6Al-4V$	115	4515	44.57

3.1 Validation of the model

Two examples of homogenous pipe vibration resting on the Pasternak Foundation were employed to prove the accuracy of the method utilized in this paper. The governing equation of this structure is as follows:

$$EI\frac{\partial^4 w}{\partial x^4} + \left(m_f + \rho A\right)\frac{\partial^2 w}{\partial t^2} + 2m_f u\frac{\partial^2 w}{\partial x\partial t} + m_f u^2\frac{\partial^2 w}{\partial x^2} + k_w w - k_p\frac{\partial^2 w}{\partial x^2} = 0 \tag{22}$$

The first example considers a pipe carrying fluid without a foundation experiencing transverse vibrations, is considered. The results for the first three vibrational modes are compared with those obtained using the semi-analytical solution DQM [37], as shown in Figure 2. In the second example, the complex eigenvalues of the first three modes of the homogeneous pipe on an elastic foundation are compared with the DTM solution presented by [9], as illustrated in Figure 3. The findings of this study align well with those reported in the previously mentioned literature.

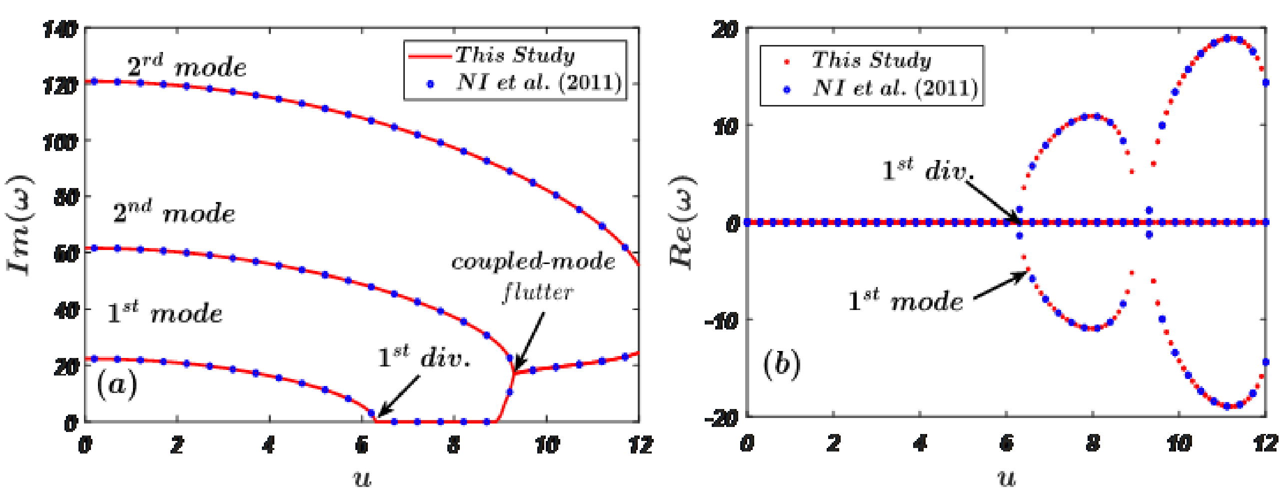

Figure 2: First three modes of dimensionless frequency versus fluid velocity (u) of pipe conveying fluid

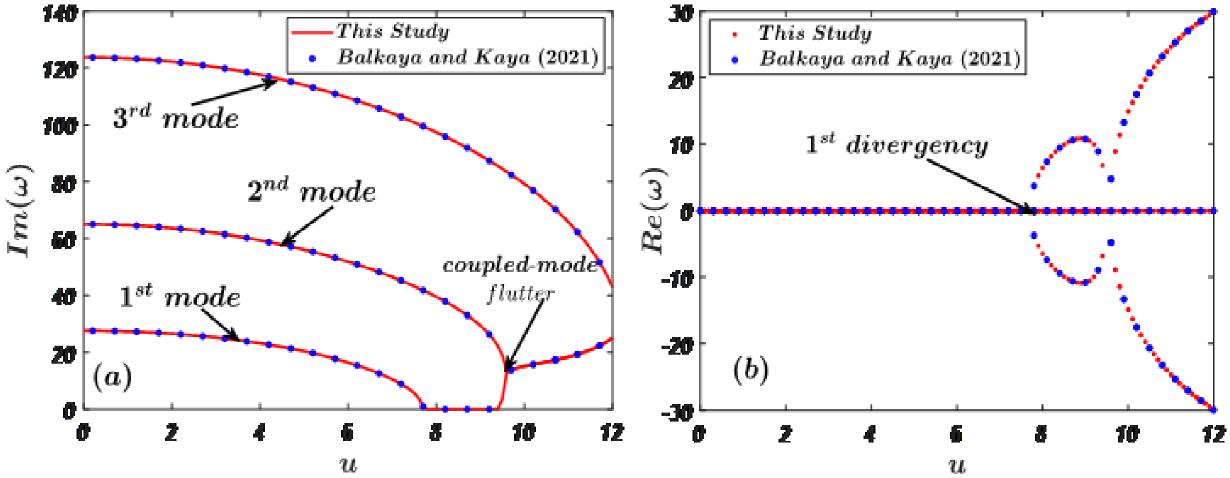

Figure 3: Real and imaginary parts of the three-mode frequencies for a classical pipe carrying fluid resting on two elastic foundations. $(k_w = 200, k_g = 3)$.

3.2 Effect of fluid flow velocity

The impact of flow velocity on the first four-mode vibration of the uniform porosity AFGM pipe, which conveys fluid under clamped-clamped (C-C) boundary conditions, is presented in this subsection, as shown in Table 2 and Figure 4. The table indicates that dimensionless velocity inversely affects the first three natural frequencies, meaning that the frequencies decrease as the velocity increases and vice versa. As the flow velocity increased, the pipe stiffness decreased, resulting in a drop in natural frequencies. In the calculation, the parameters used here are: $\beta = 0.4,\ \lambda = 0.2,\ \rho = 1, \alpha_E = 1.5, k_w = 10, and\ \ k_g = 10$.

Table 2: Influence of variable flow velocity on dimensionless vibration frequency.

Mode No.	Dimensionless flow velocity u				
	0	0.5	1	2	3
ω_1	27.5885	27.5201	27.3137	26.4788	25.0504
ω_2	72.2503	72.1747	71.9478	71.0373	69.5091
ω_3	138.5567	138.4765	138.2360	137.2718	135.6578
ω_4	226.6677	226.5852	226.3375	225.3454	223.6877

Figure 4 presents the complex parts of the first three modes of a uniform porosity AFG pipe as a function of fluid velocity. Many phenomena emerge with increasing fluid velocity, including the divergence of the first mode—where the $Im(\omega)$ of the first mode becomes zero—at a specific velocity known as the buckling critical speed, as well as coupling between the 1st and 2nd modes and between the 2nd and 3rd modes at distinct velocities. The divergence of the 1st mode occurs at u=7.04, while the coupling between the first and second frequency is observed at u=9.77. Once the $Im(\omega)$ of the 1st and 2nd frequencies merge, their real parts diverge into two branches, leading to flutter instability at u=9.77. Moreover, when u=12.54, the 2nd and 3rd modes are coupled, indicating the second flutter speed.

3.3 Power-Index (k) Influence

This subsection illustrates the impact of the material gradient on the vibration frequency of AFGM porosity pipe. The dimensionless frequencies for various gradient indices (k) are shown in Table 3 for $\beta = 0.4,\ \lambda = 0.2,\ \alpha_\rho = 1, \alpha_E = 1, k_w = 10,\ and\ k_g = 10$.The table indicates that the non-dimensional frequency drops as the material index k rises. The reduction in frequency is caused by a decrease in the proportion of ceramic material within the pipe as the gradient index increases.

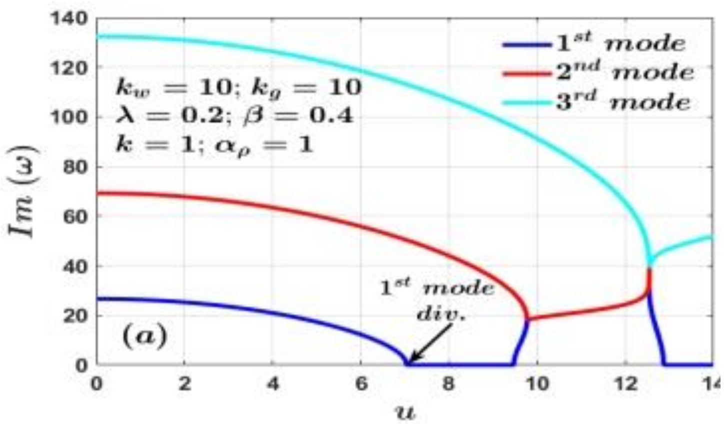

Figure 4: First three-mode vibration frequency versus flow velocity, (a) imaginary, (b) real part frequencies.

Table 3: First four dimensionless vibration frequencies at different power indices.

Freq. No	Power index					
	0	0.5	1	2	5	10
ω_1	29.4659	28.3821	27.3137	25.6274	24.2504	24.5909
ω_2	78.3052	74.7394	71.9478	68.5571	65.2025	64.1020
ω_3	151.1182	143.5160	138.236	132.4846	126.6984	123.8563
ω_4	247.9765	234.8462	226.3375	217.5035	208.6326	203.9705

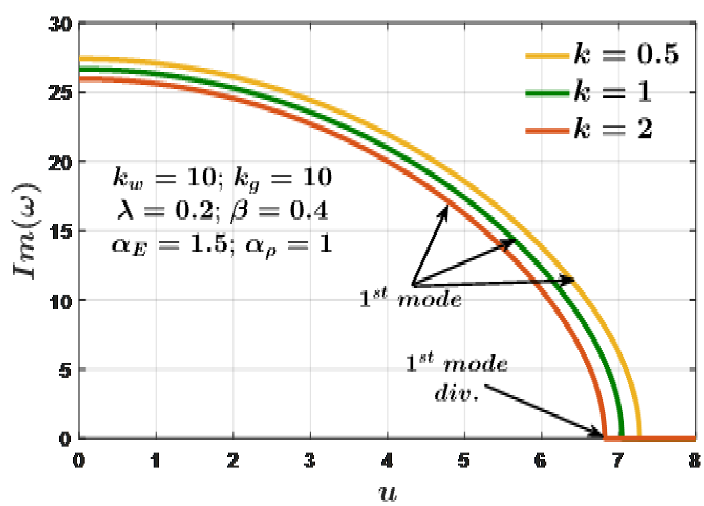

Figure 5: Variation in first-order frequency of an 'Axially functionally graded' pipe with different gradient indices.

3-4 Effect of modules of elasticity ratio α_E

This subsection discusses the impact of the modulus ratio (α_E) on the natural non-dimensional frequencies as illustrated in Table (4) for $\beta = 0.4,\ \lambda = 0.2,\ \alpha_\rho = 1,\ k_w = 10, and\ k_g = 10$. It is clear from Table 4 that when $\alpha_E < 1,$ the natural frequency increased with the growth of the gradient index, and when $\alpha_E = 1,$ the natural frequency is constant because the pipe has a homogenous material in any position of the pipe; otherwise, the trend is vice versa when $\alpha_E > 1.$

In Figure 6, the fundamental two-order frequency variations are plotted against changes in the flow velocity with two variables of modulus ratio (α_E) ($\alpha_E = 0.5\ and\ \alpha_E = 1.5$). As can be seen, the system's fundamental frequency decreases uniformly with an increase in axial velocity. In the presence of axial divergence velocity (u_d), the fundamental frequency drops to zero, after which the system undergoes divergence within a specific range of axial velocities. Thus, it is noted that as the elastic modulus ratio increases, both the 1st order frequency and the divergence system velocity also rise. This phenomenon can be attributed to the primary effect of the elastic modulus on the pipe's stiffness matrix. Thus, raising the elastic parameter enhances the pipe stiffness. Accordingly, as the modulus ratio increments, the system's divergence resistance improves, leading to higher divergence speeds. Therefore, a stiffer system is produced by increasing the elastic modulus parameter.

Table 4: Natural frequencies for different power- index k and elastic modulus ratio.

α_E	Mode No.	*Gradient index* (k)					
		0	0.5	1	2	5	10
0.25	1	15.4985	18.4943	20.9098	23.9355	25.8325	25.1425
	2	37.0364	46.7560	52.7277	59.3624	65.4105	66.5131
	3	67.5302	87.6213	98.5367	110.2291	122.0907	126.3627
0.5	1	19.1475	20.8159	22.2684	24.1976	25.5022	25.0616
	2	48.2263	53.5931	57.1811	61.2633	65.1659	66.0139
	3	90.6497	101.8173	108.3971	115.4504	122.7603	125.6864
1	1	24.8531	24.8531	24.8531	24.8531	24.8531	24.8531
	2	65.0332	65.0332	65.0332	65.0332	65.0332	65.0332
	3	124.6093	124.6093	124.6093	124.6093	124.6093	124.6093
2	1	33.4464	31.5499	29.6534	26.4689	23.7043	24.2860
	2	89.6314	83.3374	78.2284	71.8343	65.5456	63.2409
	3	173.6253	160.1122	150.3110	139.4763	128.8132	123.3688
4	1	46.0436	41.9787	37.9609	30.0735	22.0135	22.8274
	2	125.0653	111.3522	99.5001	83.1521	67.5977	60.5932
	3	243.6828	213.8140	190.1100	162.2850	136.6148	123.0693

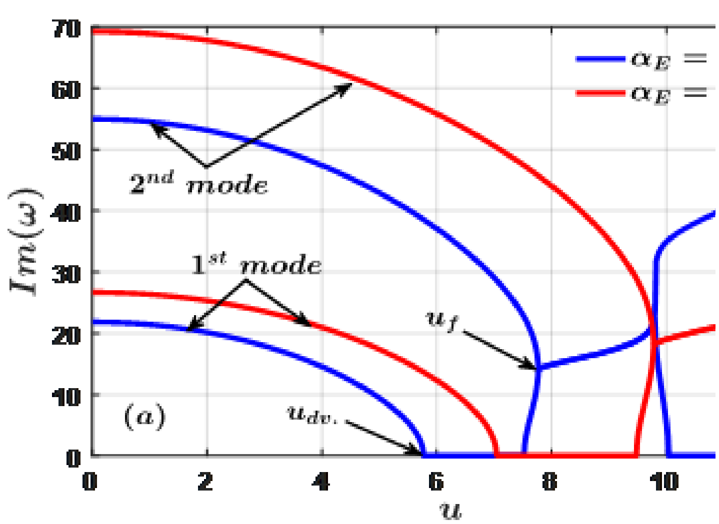

Figure 6: Effect of modulus ratio on first and second-order frequencies at various flow velocities.

3-5 Impact of foundation parameter

The fundamental frequencies of double-clamped functionally graded (FG) pipes carrying fluids are examined in this subsection for various foundation parameters $(k_w \; and \; k_g)$ as shown in Figures (7a and 7b). These figures show that a rise in coefficient foundation leads to an increase in fundamental frequencies. It can also be seen that, compared to the elastic (k_w) layer, the shear (k_g) layer has a more pronounced effect on the system's stability.

Figure 8 illustrates the effects of foundation coefficients on the static instability boundaries in the $(\omega - u)$ plane. Adding the foundation to the system enhances its effective stiffness, thereby increasing stability compared to a system without a foundation. This improvement is attributed to the stiffness matrix coefficients; as the foundation parameters increase in strength, the system's stiffness rises, resulting in greater stability. It can be seen that when increasing $(k_w \; and \; k_g)$, the FG pipe stiffness and the critical flow velocity increase. Also, this figure shows that the dimensionless frequency reduces as fluid velocity grows.

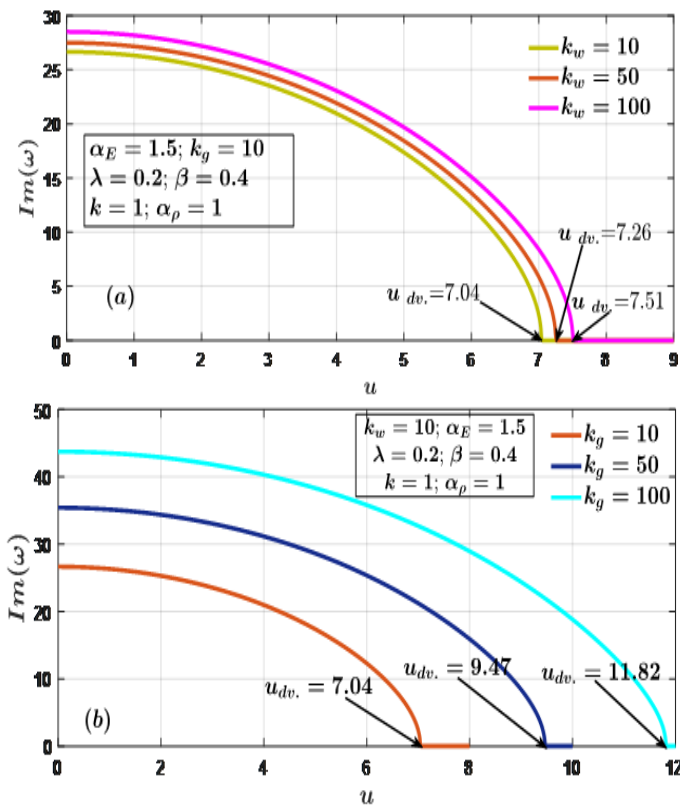

Figure 7: Influence of fluid velocity on the fundamental frequency relative to the elastic foundation parameters; (a) Winkler parameter (k_w); (b) Shear parameter (k_g).

Conclusions

This paper explores the stability of uniform porosity (AFG) pipe translating fluid. Material properties of the pipe exhibit a power-law distribution along the axial direction, and the pipe was modelled using the Euler-Bernoulli theory (EBT). Numerical simulations are conducted using the Galerkin method, and the results are confirmed by comparison with existing literature. This article investigates the pipe's dynamic behaviour concerning the FG material characteristics and various parameters. Based on this analysis, the following conclusions were drawn:

1- When the modulus ratio (α_E) is less than 1, an increase in the power index (k) results in a rise in frequency. In addition, when (α_E) is greater than 1, an increase in (k) leads to a decrease in frequency. No change in frequency is observed when (α_E) equals 1.

2- Both parameters of Pasternak's foundation $(k_w \; and \; k_g)$ enhance the pipe's dynamic characteristics.

3- The AFG pipe remains stable at low flow velocities, but its stability deteriorates as the internal fluid velocity increases. When the flow velocity surpasses a critical threshold, the pipe experiences divergence instability.

4- In AFG pipes, the fundamental frequency and divergence velocity for structural stability increment as the elastic modulus ratio (α_E) increases.

Moreover, some of the new results presented in this study could be used to control the dynamics of fluid-conveying AFG pipes since the critical flow velocities and stability regions depend on foundation parameters, gradient indexes, and porosities.

Conflict of interests

We declare that the publication of this paper does not involve a conflict of interest.

Author Contribution

Both authors were equally involved in the research design and implementation, the analysis of the results, and the writing.

Funding

There was no financial support for the authorship and publication of this article.

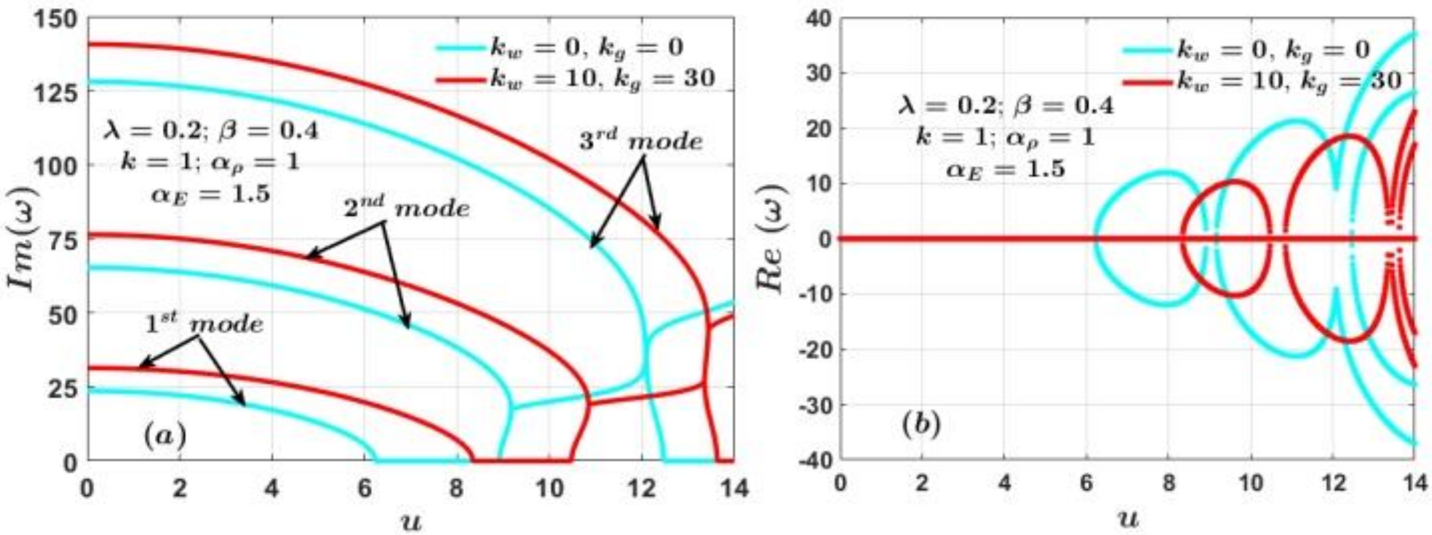

Figure 8: first three modes of fluid conveying AFG pipe with and without elastic foundation.

Nomenclature

Symbol	Definition
A	Cross-sectional area (m²)
AFG	axially functionally graded
C-C	Clamped-Clamped
DTM	Differential transformation method
E	Modulus of elasticity GPa
FEM	Finite element method
G	Modulus of rigidity GPa
HDQ	Harmonic differential quadrature
I	Second moment of inertia m4
k	Volume fraction index
k_g	Dimensionless shear parameter
k_W	Dimensionless elastic parameter
L	Pipe length m
m_f	Fluid mass per unit length kg. L-1
r_i	Inner radius mm
r_o	Outer radius mm
T	Kinetic Energy m-kg-s
t	Time s.
U	Fluid velocity m.s-1
U_S	Strain Energy m-kg-s
W	Virtual work m-kg-s

References

[1] Heshmati, M., Daneshmand, F. & Amini, Y. Vibration and stability analysis of functionally graded elliptical pipes conveying fluid with flow velocity profile modification. Engineering with Computers, **39**, 1537–1552 (2021).

[2] Giacobbi, D. B., Semler, C. & Païdoussis, M. P. Dynamics of pipes conveying fluid of axially varying density. Journal of Sound and Vibration **473**, 115202 (2020).

[3] Dagli, B. Y. & Ergut, A. Dynamics of fluid conveying pipes using Rayleigh theory under non-classical boundary conditions. *Eur. J. Mech. B/Fluids* **77**, 125–134 (2019).

[4] Xu, Y. *et al.* Nonlinear dynamics of viscoelastic fluid-conveying pipe installed within uniform external cross flow by pipe clamps. *Appl. Ocean Res.* **135**, 103547 (2023).

[5] Zhao, Q., Liu, W., Yu, W. & Cai, F. Dynamics of a Fluid-Conveying Pipe by a Hybrid Method Combining Differential Transformation and Galerkin Discretization. *Iran. Journal Sci. Technol. - Trans. Mech. Eng.* **48**, 647–659 (2024).

[6] Ma, Y., You, Y., Chen, K. & Feng, A. Analysis of vibration stability of fluid conveying pipe on the two-parameter foundation with elastic support boundary conditions. *J. Ocean Eng. Sci.* (2022) doi:10.1016/j.joes.2022.11.002.

[7] Li, M., Zhao, X., Li, X., Chang, X. P. & Li, Y. H. Stability analysis of oil-conveying pipes on two-parameter foundations with generalized boundary condition by means of Green's functions. *Engineering Structure* **173**, 300–312 (2018).

[8] Askarian, A. R., Permoon, M. R. & Shakouri, M. Vibration analysis of pipes conveying fluid resting on a fractional Kelvin-Voigt viscoelastic foundation with general boundary conditions. *Int. J. Mech. Sci.* **179**, 105702 (2020).

[9] Balkaya, M. & Orhan Kaya, M. Analysis of the instability of pipes conveying fluid resting on two-parameter elastic soil under different boundary conditions. *Ocean Eng.* **241**, 110003 (2021).

[10] Wu, N., Zhao, Y., Guo, Q. & Liu, Y. The effect of two parameters of Pasternak foundations on the dynamics and stability of multi-span pipe conveying fluids. *Adv. Mech. Eng.* **12**, 1–7 (2020).

[11] Saleh, B. *et al.* 30 Years of functionally graded materials: An overview of manufacturing methods, Applications, and Future Challenges. *Compos. Part B Eng.* **201**, 108376 (2020).

[12] Elaikh, T. E., Abd, N. M. & Ali, A. H. Dynamic characteristics of cracked simply supported bidirectional functionally graded Rayleigh beam. *Results Mater.* **19**, 100441 (2023).

[13] Jha, D. K., Kant, T. & Singh, R. K. A critical review of recent research on functionally graded plates. *Compos. Struct.* **96**, 833–849 (2013).

[14] Awrejcewicz, J., Kurpa, L. & Shmatko, T. Linear and nonlinear free vibration analysis of laminated functionally graded shallow shells with complex plan form and different boundary conditions. *Int. J. Non. Linear. Mech.* **107**, 161–169 (2018).

[15] Cao, J. Instability Analysis of Fluid-Conveying Functionally Graded Thin-Walled Pipes on Random Elastic Foundations. *J. Phys. Conf. Ser.* **2230**, (2022).

[16] Ma, T. & Mu, A. Analysis of Nonlinear Vibration of Functionally Graded Simply Supported Fluid-Conveying Microtubes Subjected to Transverse Excitation Loads. *Micromachines* **13**, (2022).

[17] Guo, Q., Liu, Y., Chen, B. & Zhao, Y. An efficient stochastic natural frequency analysis method for axially varying functionally graded material pipe conveying fluid. *Eur. J. Mech. A/Solids* **86**, 104155 (2021).

[18] Ihmood, S. M., Elaikh., T. E. & Al-Umar, M. Free vibration of new type functionally graded materials pipe conveying fluid using differential quadrature method. *AIP Conf. Proc.* **2386**, (2022).

[19] R. B, E., EH. Elaikh, T. & . M.H, S. Differential Quadrature Method for Dynamic behavior of Function Graded Materials pipe conveying fluid on a visco-elastic foundation. *Univ. Thi-Qar J. Eng. Sci.* **10**, (2019).

[20] Selmi, A. & Hassis, H. Vibration analysis of post-buckled fluid-conveying functionally graded pipe. *Compos. Part C Open Access* **4**, 100117 (2021).

[21] Deng, J., Liu, Y., Zhang, Z. & Liu, W. Stability analysis of multi-span viscoelastic functionally graded material pipes conveying fluid using a hybrid method. *Eur. J. Mech. A/Solids* **65**, 257–270 (2017).

[22] Wang, Z. M. & Liu, Y. Z. Transverse vibration of pipe conveying fluid made of functionally graded materials using a symplectic method. *Nucl. Eng. Des.* **298**, 149–159 (2016).

[23] An, C. & Su, J. Dynamic Behavior of Axially Functionally Graded Pipes Conveying Fluid. *Math. Probl. Eng*, (2017).

[24] Zhao, Y., Hu, D., Wu, S., Long, X. & Liu, Y. Dynamics of axially functionally graded conical pipes conveying fluid. *J. Mech.* **37**, 318–326 (2021).

[25] Elaikh, T. E. H., Abed, N. M. & Ebrahimi-Mamaghani, A. Free Vibration and Flutter Stability of Interconnected Double Graded Micro Pipes System Conveying Fluid. *IOP Conf. Ser. Mater. Sci. Eng.* **928**, (2020).

[26] Zhu, B., Chen, X. C., Guo, Y. & Li, Y. H. Static and dynamic characteristics of the post-buckling of fluid-conveying porous functionally graded pipes with geometric imperfections. *Int. J. Mech. Sci.* **189**, 105947 (2021).

[27] Li, N., Zhang, H. & Bai, C. Effects of pores on nonlinear vibration and post-buckling behavior of functionally graded material pipes conveying fluid. *Proc. Inst. Mech. Eng. Part C J. Mech. Eng. Sci.* **237**, 4187–4202 (2023).

[28] Zhou, J., Chang, X. & Li, Y. Nonlinear vibration analysis of functionally graded flow pipelines under generalized boundary conditions based on homotopy analysis. *Acta Mech.* **233**, 5447–5463 (2022).

[29] Khodabakhsh, R., Saidi, A. R. & Bahaadini, R. Exact Closed-Form Solution for Nonlinear Stability Analysis of Porous Functionally Graded Pipes Conveying Fluid Under Various Boundary Conditions. *J. Vib. Eng. Technol.* **10**, 2877–2891 (2022).

[30] Mao, X. Y., Jing, J., Ding, H. & Chen, L. Q. Dynamics of axially functionally graded pipes conveying fluid. *Nonlinear Dyn.* **111**, 11023–11044 (2023).

[31] Elaikh, T. E. & Agboola, O. O. O. Investigation of Transverse Vibration Characteristics of Cracked Axially Moving Functionally Graded Beam Under Thermal Load. *Trends Sci.* **19**, (2022).

[32] Safa Ha. Majeed, Talib Eh. Elaikh, A. A. U. Reformulated Strain Gradient (Rsg) Elasticity Theory For Free Vibration Of Thermal Bi-Directional Fg Microbeam. *J. Teknol.* **2**, 123–134 (2024).

[33] Rao, S. S. *Vibration of Continuous Systems*. *Vibration of Continuous Systems* (2007). doi:10.1002/9780470117866.

[34] Ebrahimi-Mamaghani, A., Sotudeh-Gharebagh, R., Zarghami, R. & Mostoufi, N. Thermo-mechanical stability of axially graded Rayleigh pipes. *Mech. Based Des. Struct. Mach.* **1**, 1–30 (2020).

[35] Talib EH. Elaikh, N. M. A. Stability of FG material micro-pipe conveying fluid. **10**, 211–222 (2019).

[36] Zhao, Y., Hu, D., Wu, S., Long, X. & Liu, Y. Dynamics of axially functionally graded conical pipes conveying fluid. *J. Mech.* **37**, 318–326 (2021).

[37] Ni, Q., Zhang, Z. L. & Wang, L. Application of the differential transformation method to vibration analysis of pipes conveying fluid. *Appl. Math. Comput.* **217**, 7028–7038 (2011).